Status of Collider and Booster Magnets for FCC-ee

J. Bauche, C. Eriksson, *et al.*, FCC Week 2022, 1st June 2022.

Many thanks to:

D. Aguglia, A. Chance (CEA), T. Charles, B. Dalena (CEA) L. Fiscarelli, M. Karppinen, A. Milanese, K. Oide, C. Petrone, D. Schoerling, R. Tomas Garcia, E. Todesco, D. Tommasini, and other members of the FCC collaboration.

Outline

Collider magnets

- **Dipole mechanical design**
- **Quadrupole magnetic axis shift**

Booster magnets

- **Magnet specifications**
- **Dipole design**

Magnet work package

- **Collaborations**

Conclusions

References

Collider Magnets

Dipole magnetic design

- Twin aperture design, magnetically coupled [1], [2]
- Simple, pure, **cost effective**
- **Low power consumption** (50% w.r.t. separate magnets)
- **300 mm inter-beam distance** shared between vacuum chamber, SR absorbers, busbars and yoke return leg
- DC operation, compatible with solid iron yoke construction, but alternatives are possible
- Twin air-cooled aluminium busbar considered in CDR, modified to **single water-cooled busbar**

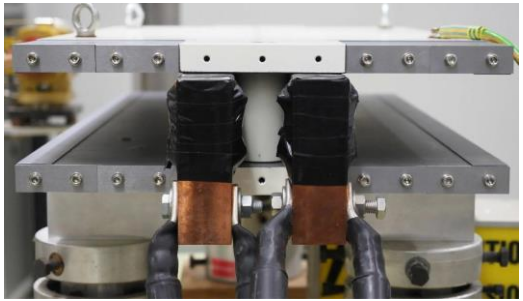

Prototype 1m-long, single busbar "coil", measurements reported in [3]

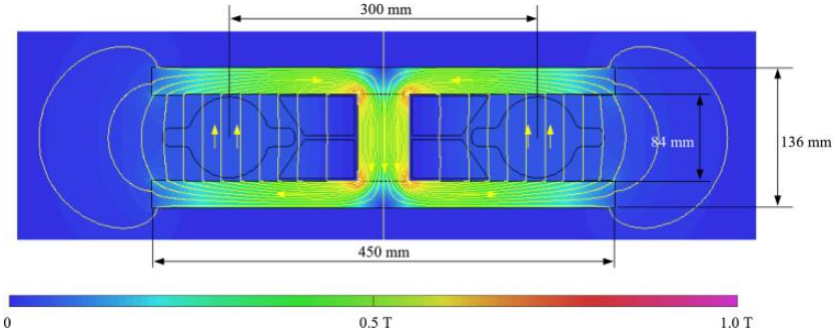

Magnetic model cross-section (CDR), B_0 max = 57 mT

Strength, 45.6 GeV–182.5 GeV	mT	14.1–56.6
Magnetic length	m	21.94/23.94
Number of units per ring		2900
Aperture (horizontal × vertical)	mm	130 × 84
Good field region (GFR) in horizontal plane	mm	±10
Field quality in GFR (not counting quadrupole term)	10^{-4}	≈1
Central field	mT	57
Expected b_2 at 10 mm	10^{-4}	≈3
Expected higher order harmonics at 10 mm	10^{-4}	¡1
Maximum operating current	kA	1.9
Maximum current density	A/mm^2	0.79
Number of busbars per side		2
Resistance per unit length (twin magnet)	μΩ/m	22.7
Maximum power per unit length (twin magnet)	W/m	164
Maximum total power, 81.0 km (interconnections included)	MW	13.3
Inter-beam distance	mm	300
Iron mass per unit length	kg/m	219
Aluminium mass per unit length	kg/m	19.9

Parameters (CDR) [1]

Dipole mechanical design

Yoke assembly scheme

- Baseline design: top-bottom yoke assembly via interleaved **columns**
- Creates dilution and improve μ_r working point of yoke back leg
- **Tight tolerances** needed to ensure field quality

→ ***Costly*** *for large scale production (~ 700,000 columns for the whole ring…)*

→ *Low mechanical inertia → significant magnet* ***sag*** *→ strong reinforcement needed*

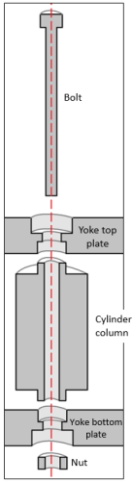

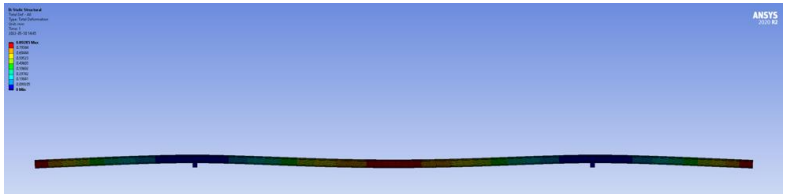

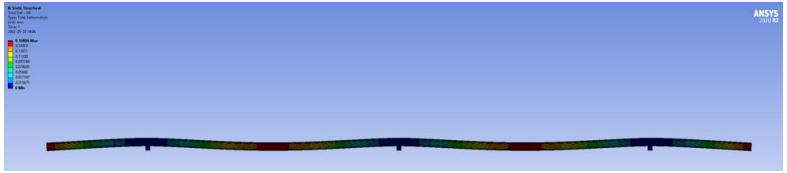

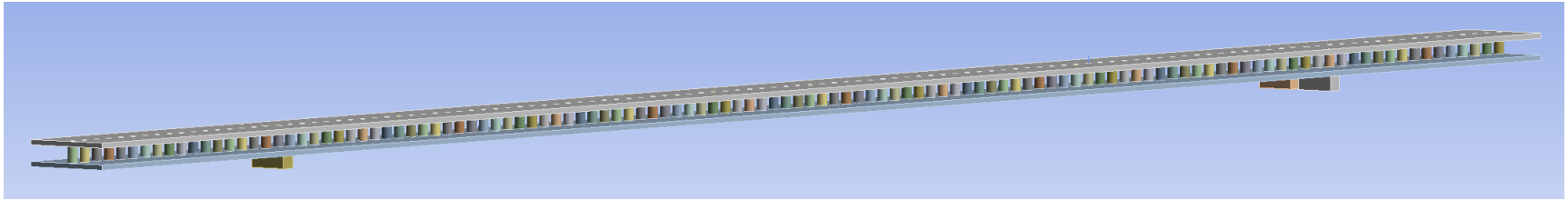

12 m long dipole, 120 columns

New yoke assembly scheme

- New design considered with continuous beam of sandwich material (iron – aluminium – iron) to preserve dilution effect
  - → ***Easier*** *and* ***cheaper*** *to produce*
  - → *Dilution rate to be optimized with electromagnetic simulations*
  - → *Preliminary 2D results do not show any significant effect on field quality*

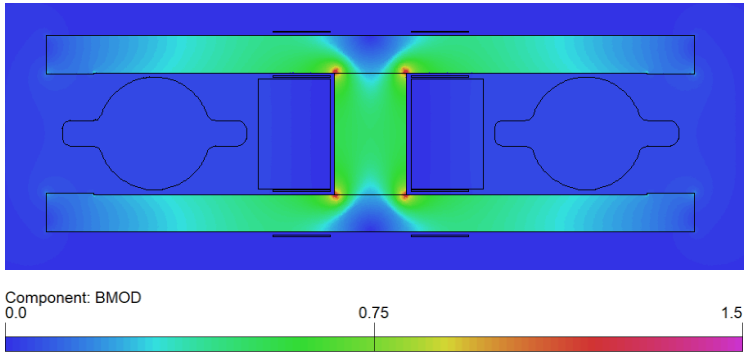

B_{mod}, column assembly (FEM 2D)

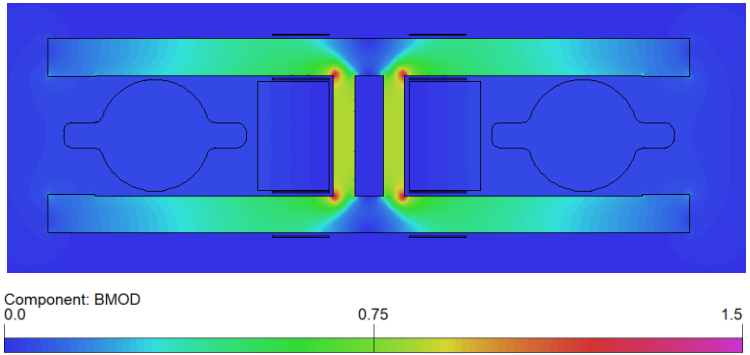

B_{mod}, sandwich assembly (FEM 2D)

Dipole supporting scheme (for 12 m long units)

- The new design with continuous beam of sandwich material performs much better in sag
- It does not require additional reinforcement

→ ***3 supporting points*** *to limit sag to* ***< 0.5 mm***

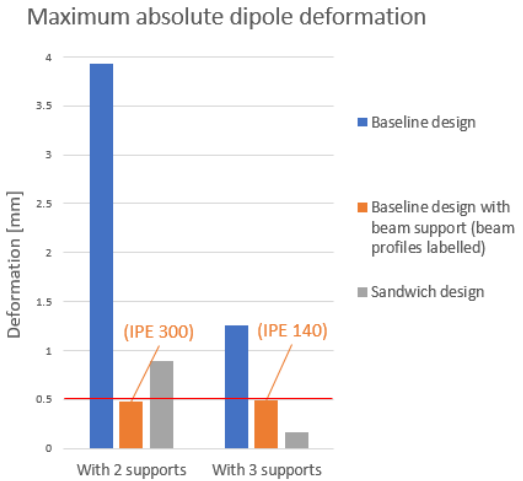

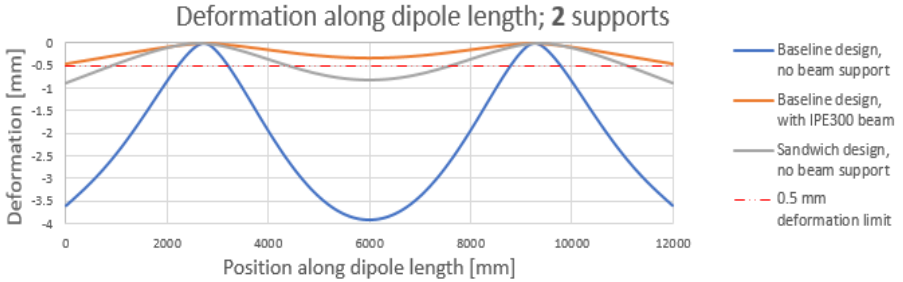

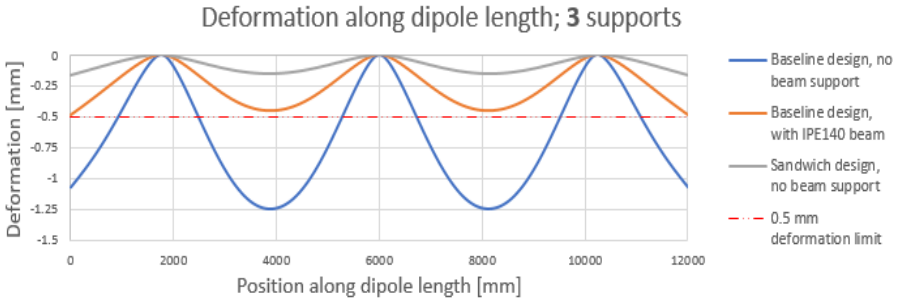

Simulated 12 m long magnet sag with 2 and 3 supports (ANSYS)

Interconnections

- Vacuum chamber interconnection between dipoles presently foreseen with flanges
  - → *Dimensions **not fitting in magnet aperture**, design in progress*
  - → *Routing of busbars around flanges would impact on **interconnection length** (machine performance, cost, reliability)*
  - → *With **smaller flanges** fitting in aperture **"covering" interconnection with B field** can be considered*
- **No space reservation** for **SR absorbers** in present cross-section design (require strong water cooling)
  - → ***Magnet cross section might need redesign***
  - → ***Inter-beam distance might have to be increased***

➔ **Detailed design studies to be performed**

(see C. Garion talk)

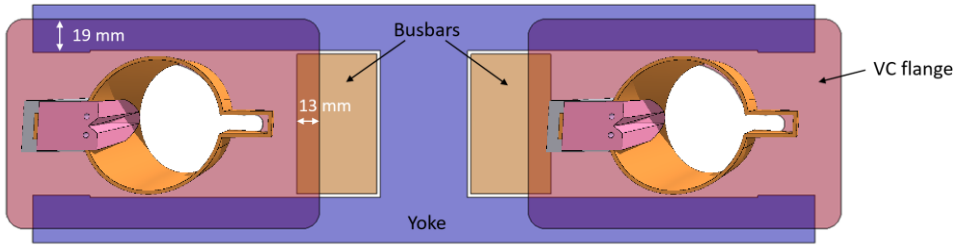

Integration of vacuum flanges and SR absorbers in dipole cross section

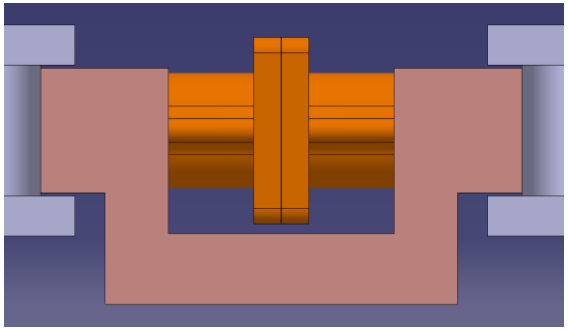

Schematic busbar routing around flanges

Quadrupole magnetic design

- Twin aperture design, magnetically coupled [1], [2]
- Only **2 racetrack coils** for 8 poles, out of mid-plane (SR)
- **Low power consumption** (50% w.r.t. separate magnets)
- Top-bottom assembly via non-magnetic central spacer
- Equilibrium of **parallel flux distribution** between horizontal and vertical field lines controlled by central gap height (adjustable with end shims on prototype
- ~10x higher flux density than in dipoles; water-cooled coil (optimization of dipole filling factor)

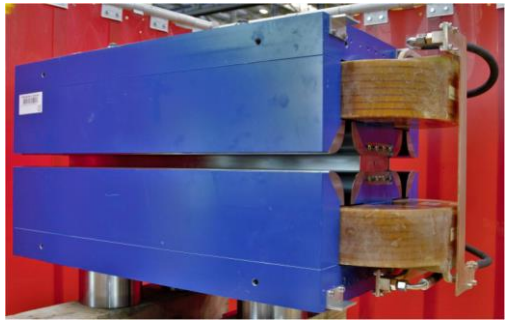

Prototype 1m-long

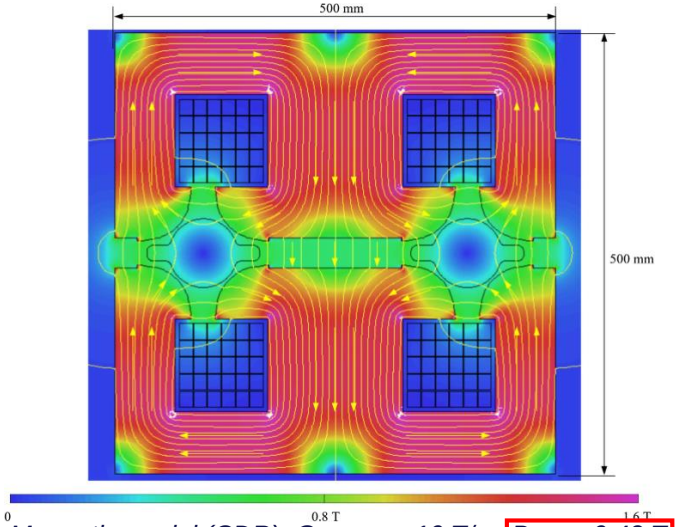

Magnetic model (CDR), G_0 max = 10 T/m, $B_{pole\ tip}$ 0.42 T

Maximum gradient	T/m	10.0
Magnetic length	m	3.1
Number of twin units per ring		2900
Aperture diameter	mm	84
Radius for good field region	mm	10
Field quality in GFR (not counting dip. term)	10^{-4}	≈1
Maximum operating current	A	474
Maximum current density	A/mm^2	2.1
Number of turns		2 × 30
Resistance per twin magnet	mΩ	33.3
Inductance per twin magnet	mH	81
Maximum power per twin magnet	kW	7.4
Maximum power, 2900 units (with 5% cable losses)	MW	22.6
Iron mass per magnet	kg	4400
Copper mass per magnet (two coils)	kg	820

Parameters (CDR)

Quadrupole magnetic axis shift

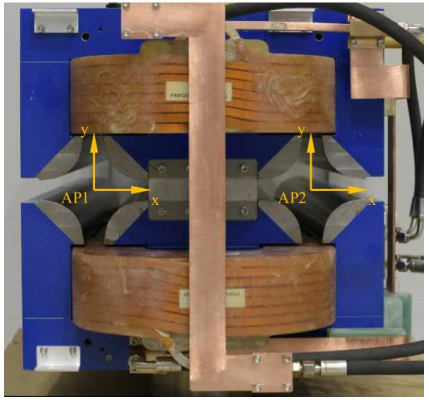

Magnetic measurements performed on 1-m prototype [3]

- ~0.4 mm shift for each aperture between low and high fields
- Mismatch MM vs. FEM (3D) at low fields not completely explained

➔ To be further investigated

DIPOLE AND SEXTUPOLE COMPONENTS IN THE TWIN QUADRUPOLE

I [A]	x_{ctr} [mm]			$\int b_3$ [10^{-4} @ 10 mm]		
	AP1	AP2	FEM	AP1	AP2	FEM
25	0.75	-0.75	0.17	13.1	-14.4	-57.9
50	0.22	-0.23	0.17	34.7	-35.4	-57.9
100	-0.07	0.07	0.17	46.6	-46.6	-58.0
150	-0.17	0.16	0.17	50.9	-50.9	-58.2
200	-0.22	0.22	0.18	53.5	-53.6	-59.0
250	-0.29	0.27	0.22	57.8	-57.2	-62.5
200	-0.23	0.22	0.18	53.1	-53.3	-59.0
150	-0.18	0.17	0.17	51.0	-50.6	-58.2
100	-0.10	0.09	0.17	46.9	-46.9	-58.0
50	0.15	-0.16	0.17	35.7	-35.2	-57.9
25	0.59	-0.59	0.17	15.9	-14.9	-57.9

The simulation results are for AP2, as ¼ of the magnet is modeled; furthermore, no hysteretic behavior is considered in the BH curve.

Measured magnetic axis shift and ∫b3

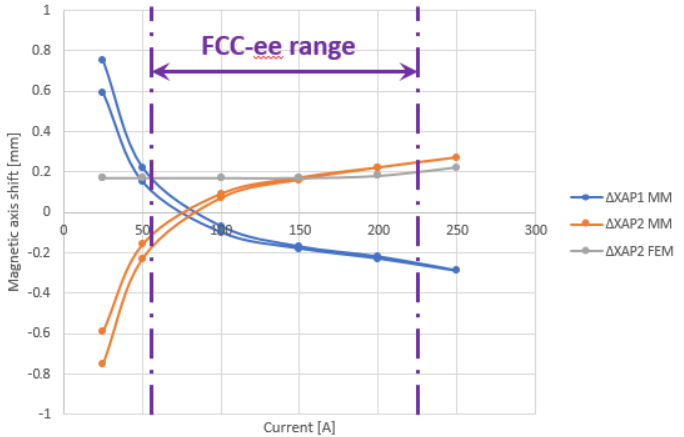

Magnetic axis shift

Quadrupole field tapering

Trim coils

- Needed on each aperture for **individual aperture trimming**
- Gradient trim effect only on concerned aperture
- Significant **cross-talk** : both **magnetic axes shift** in same direction up to 0.2 mm @ 1.5% dB, even when single aperture trim is activated
- b_3 significantly affected in both apertures with same polarity

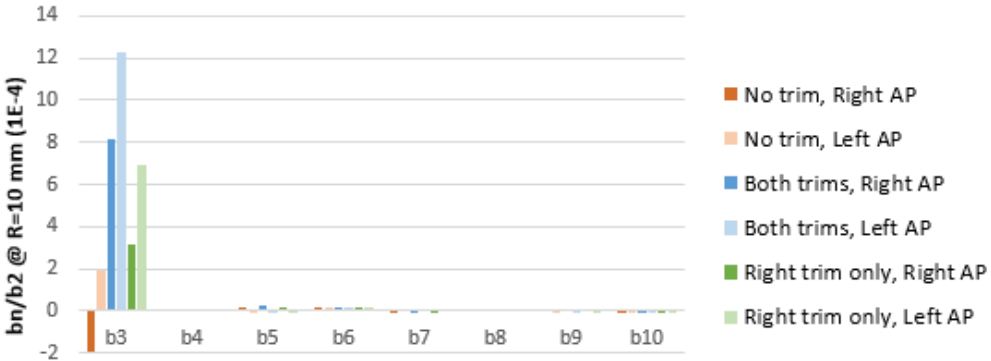

Simulated normalized harmonics (FEM 2D)
VALUES TO BE CONFIRMED BY MEASUREMENTS

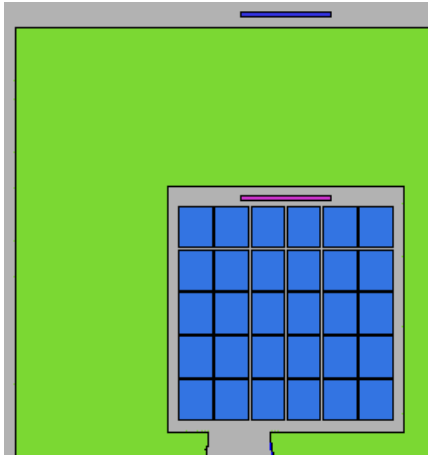

Current polarities in main and trim conductors

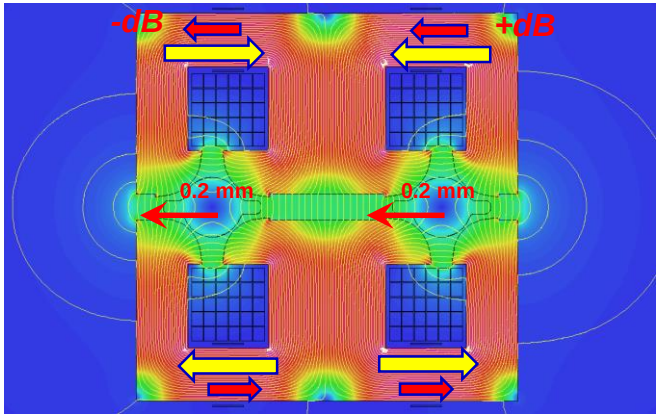

Flux density and field lines, trims activated

Alternative design

Compensation of inner/outer asymmetry

- Magnetic gap between apertures to **reduce flux jump**
- Chamfer on outer sides to **limit flux leakage**
- Magnetic axis shift and b_3 **mitigated but not suppressed**
- **To be checked** with further simulations and measurement of a new model magnet

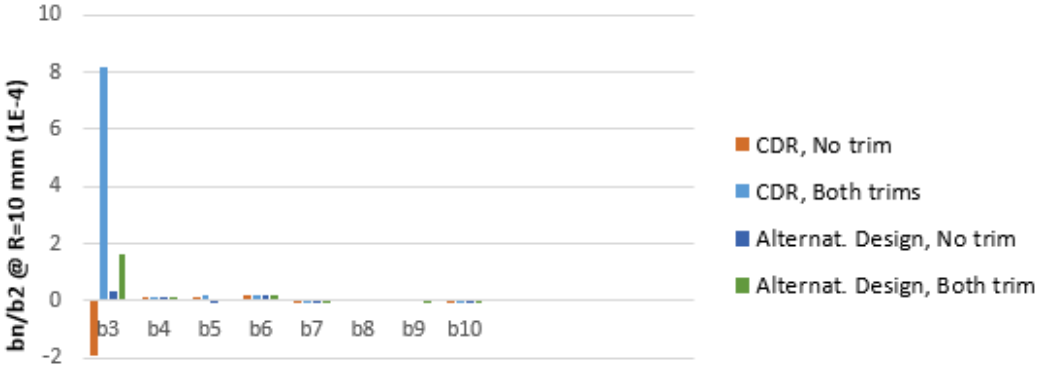

Simulated normalized harmonics (FEM 2D)
VALUES TO BE CONFIRMED BY MEASUREMENTS

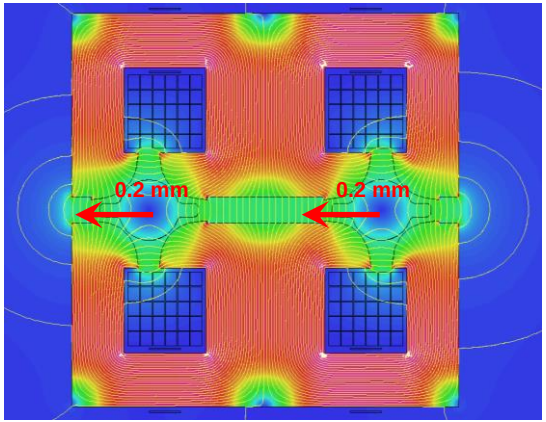

CDR design, trims activated

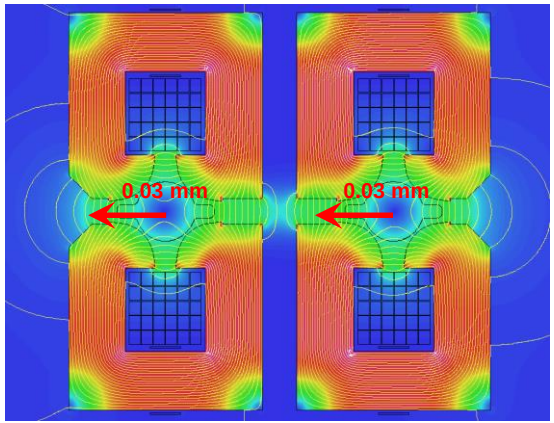

Alternative design, trims activated

Sextupole magnetic design

- Classical design as first approach for CDR
- Fits in 300 mm inter-beam distance, compatible with **individual magnets** for each beam
- "Busy" cross section, **current** and **flux densities** at **upper values, dissipated power > dipoles**
- Vacuum chamber winglets and SR absorbers **integration issue** with coils on mid-plane
- Integration of **trim circuits** (H/V orbit correctors, skew quadrupoles) to be performed
- Cross section could be relaxed with 3 fold symmetry

➔ **Design to be reworked with updated specifications**

➔ *This work is expected to be taken over by another institute member of the **FCC collaboration** (addendum to collaboration agreement in preparation)*

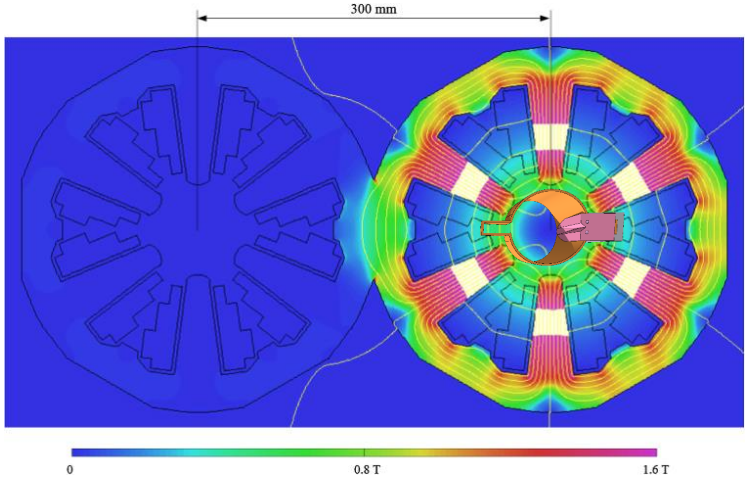

Magnetic model (CDR), S_0 max = 403.5 T/m², $B_{pole\ tip}$ 0.59 T

Maximum strength, B″	T/m²	807.0
Magnetic length	m	1.4
Number of units per ring		208×4 = 832 (Z, W) 292 × 8 = 2336 (H, tt̄)
Number of families per ring		208 (Z, W) 292 (H, tt̄)
Aperture diameter	mm	76
Radius for good field region (GFR)	mm	10
Field quality in GFR	10^{-4}	≈1
Ampere turns	A	6270
Current density	A/mm²	7.8
Maximum power per single magnet at 182.5 GeV	kW	15.5
Average power per single magnet at 182.5 GeV	kW	4.4
Total power at 182.5 GeV (4672 units)	MW	20.5

Parameters (CDR)

Booster Magnets

Magnet specifications and challenges

dipoles = 2×2944
quadrupoles = 2944
sextupoles = 2632/4

- Single aperture machine, cycled
- No field “tapering” considered for E saw tooth
- **Aperture Ø 50 mm**, GFR over 2/3 aperture, **dB/B < 1.0E-4**
- **Challenging dipole field at injection**, only ~150 x B_{earth}
- Quadrupole and sextupole designs in progress. Field levels seem to be in achievable ranges, similar to ELENA magnets [5]

→ *We will focus on the dipole design in the next slides*

Courtesy A. Chance, B. Dalena

Magnet	Parameter	Unit	Value
Dipole	Field at injection (20 GeV)	G	71
	Field at ttbar energy (182.5 GeV)	G	650
	Length	m	11.1
Quadrupole	Gradient at injection (20 GeV)	T/m	2.5
	Gradient at ttbar energy (182.5 GeV)	T/m	22.5
	Length	m	1.5
Sextupole	Gradient at injection (20 GeV)	T/m^2	174
	Gradient at ttbar energy (182.5 GeV)	T/m^2	1582
	Length	m	0.5

Booster magnet parameters

The injection energy for the booster is determined by the field quality and reproducibility of the magnetic field in the dipole magnets of the arc sections. The current design features an energy of 20 GeV, corresponding to a magnetic field of $B = 6\,\mathrm{mT}$.

CDR, Booster chapter, p. 495 [4]

Table 6.15. Booster cycle parameters.

Parameter	Unit	Z	W	H	$t\bar{t}_1$	$t\bar{t}_2$
Flat bottom duration	s	51.1	11.8	5.0	1.6	1.6
Cycle duration	s	51.7	13.3	7.5	5.5	5.7
Ramp rate up	G/s			254		

CDR, Booster cycle [4]

Dipole design

- **Main considerations for design**
  - ***Performance**: field quality, reproducibility, and limited sensitivity to perturbations (@ injection)*
  - ***Cost optimization**: large scale manufacturing, power consumption and energy storage*
  - ***Size**: integration in same tunnel as collider*

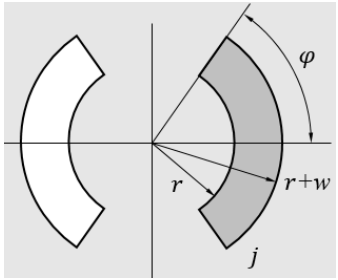

$$B = \frac{2\mu_0 \sin\varphi \; j \; w}{\pi}$$

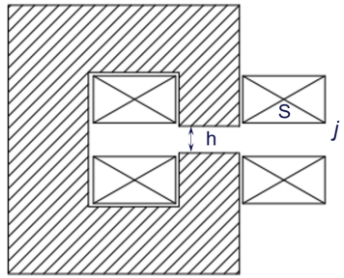

$$B = \frac{2\mu_0 \; j \; S}{h}$$

Ampere-turns >10x larger for ironless magnet for same aperture

- **Design options**

→ ***Coil dominated** magnet or **iron dominated** magnet?*

- ***Field range achievable** in normal conducting mode for both options*
- *Required **ampere-turns much larger** for **coil dominated**, even with iron shell (power consumption, capital cost, size)*
- ***Ironless** magnet does not shield the **earth magnetic field** (B_{earth} ≈ 70 units of B_{inj})* → *not acceptable*
- ***Strong sensitivity** of field quality to **coil positioning** for **coil dominated***
- *Required **conductor shape not commercially available** for **coil dominated*** → *costly for large scale manufacturing*
- *Effect of iron **coercivity** on low field performance larger for **iron dominated** magnet*

→ trial for iron dominated magnet…

- **Design options**

→ ***C-shape** magnet / **O-shape** magnet / **H-shape** magnet?*

- *As iron dominated, all magnet configurations need the **same ampere-turns** for a defined field and aperture*
- ***C-shape** provides better access to vacuum chamber*

  → *not a specific requirement for the booster*
- ***O-shape** and **H-shape** provide full shielding against magnetic perturbations (earth field) along the yoke*
- ***C-shape** and **H-shape** do not have coils in mid-plane*

  → *limited SR in booster (low beam current), to be assessed*
- ***O-shape** provides the most compact layout*

  → *easier integration of booster in collider tunnel*
- ***O-shape** naturally provides more homogeneous field for smaller pole width*

  → *reduced magnetic energy* → *smaller energy storage system (see D. Aguglia)*
- ***O-shape** naturally provides larger air-to-iron path for magnetic flux (coercivity)*

→ trial for O-shape magnet…

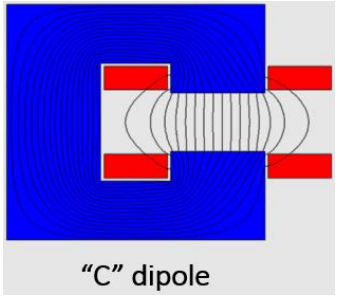

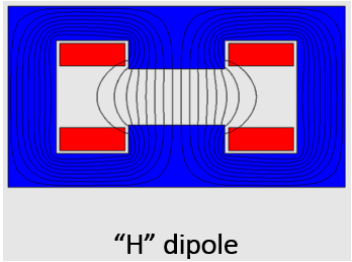

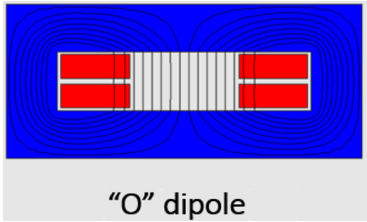

- **Driving parameters for calculations**
  - ***Bore aperture**: beam + vacuum chamber + clearance: **55 mm***
  - ***Current density**: assumed air cooled coils, aluminum: **<1 A/mm²***
  - ***Aperture width**: low pole "overhang" thanks to O-shape*
  - ***Yoke thickness**: thin for optimized μ_r but mechanically stable*
  - ***Yoke material**: laminated silicon electrical steel, no dilution, NGO: **M270-50A** (coercivity **H_c = 30 A/m** from ELENA magnets) [5]*

- **O-shape magnet**
  - *The dimensions can be very small, magnet mass **~ 62 kg/m**!*
  - *Flux density in return yoke ~ 0.5 T with 10 mm yoke thickness*
  - *Natural positive sextupole of O-shape compensated with short pole step (H-shape like) and pole shims*
  - *Field quality sensitive to coil horizontal position by **~ 1 unit / mm** (sensitivity <10x coil dominated) → achievable at reasonable cost with automatized manufacturing process (coherent with large scale production)*

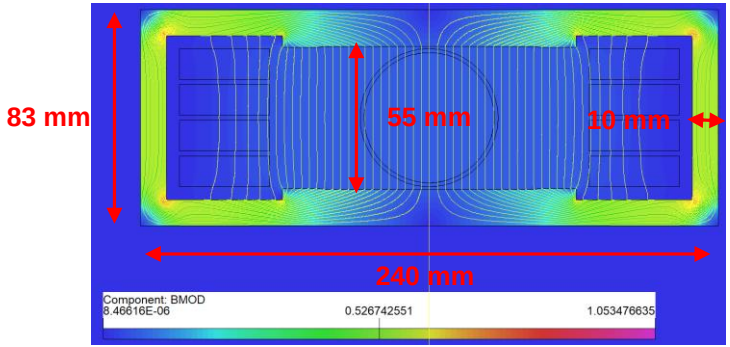

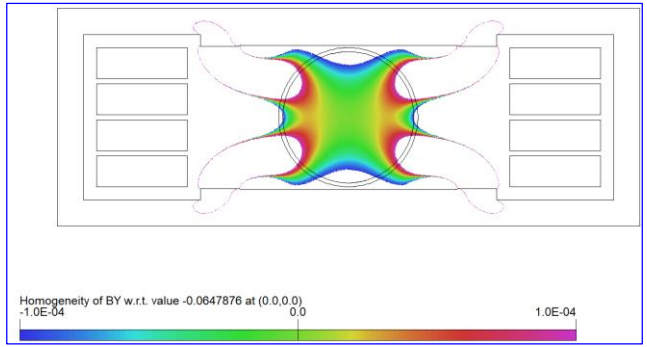

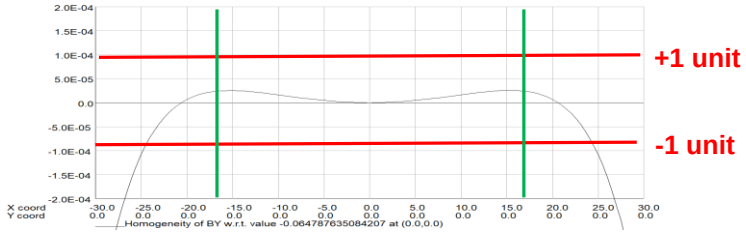

- **Effect of coercivity**
  - *Flux lines along the pole iron → different path lengths*
  - *At low fields,* $\Delta B_{rem} \propto \Delta H_c * \Delta l_{iron} / l_{air}$
  - *H_c scales with iron magnetization, ~10 times larger at tt_{bar} extraction than at injection*
  - *An "anvil" pole shape can mitigate the effect, in the spirit of the LHeC dipole [7]*
  - *Simulations incl. hysteretic behavior needed, based on steel characterization*
  - *Model magnets to test GO vs. NGO, dilution, etc.*

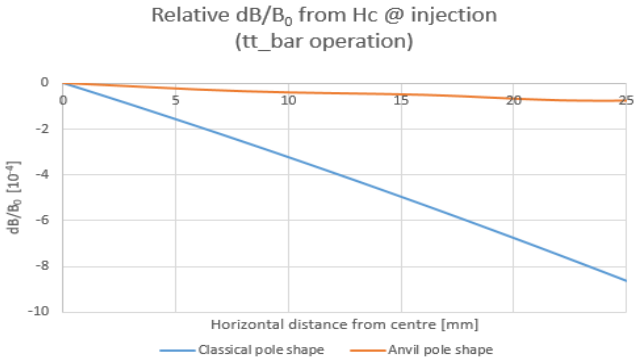

dB/B_0 from H_c (B) for FCC-ee, fit from ELENA [5] and SPS [6] data

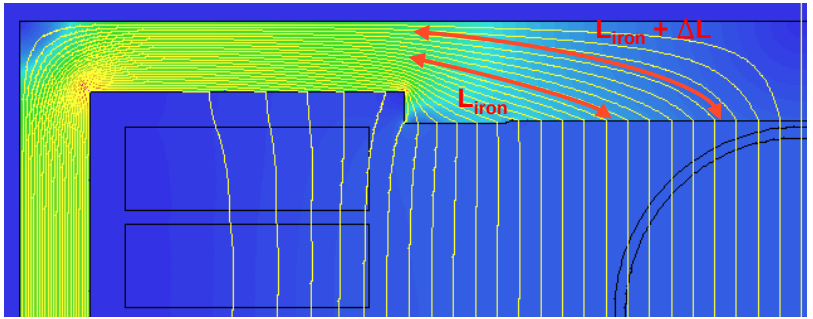

O-shape magnet

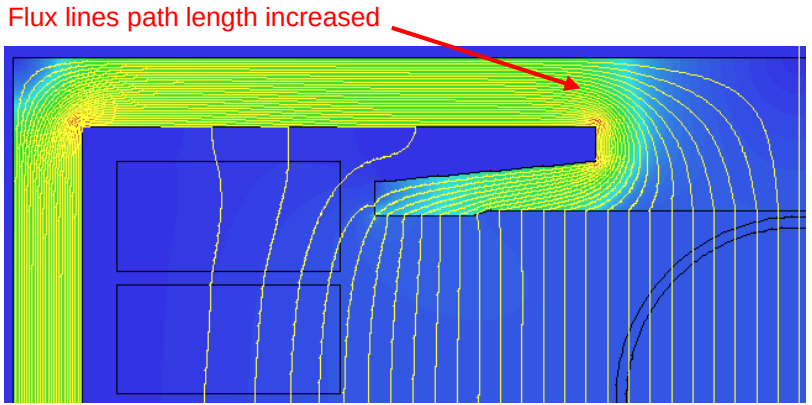

"Anvil" pole shape magnet

- **Flux density in iron**
  - ***Return yoke*** *and* ***pole edges*** *operate in regions of "better"* ***known magnetic characteristics*** *(μ_r , H_c)*
  - *In* ***pole central part****, characteristics to be* ***determined experimentally***
  - *Flux density can be modulated locally by trimming the iron*

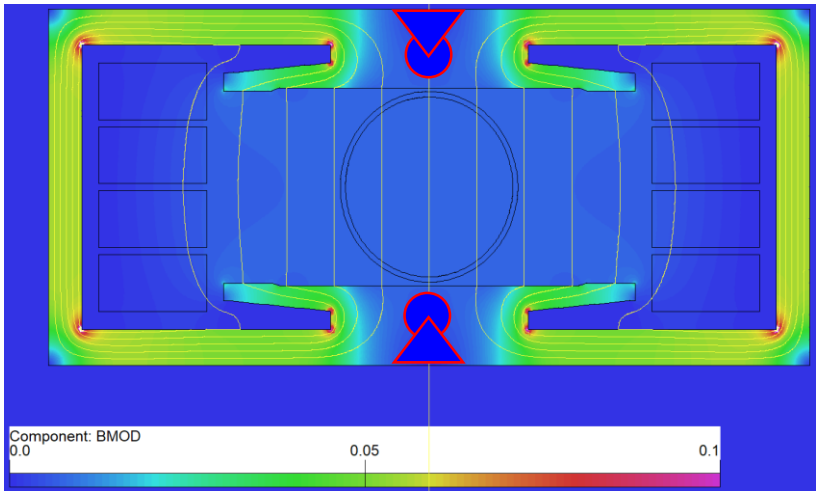

@ injection, 20 GeV

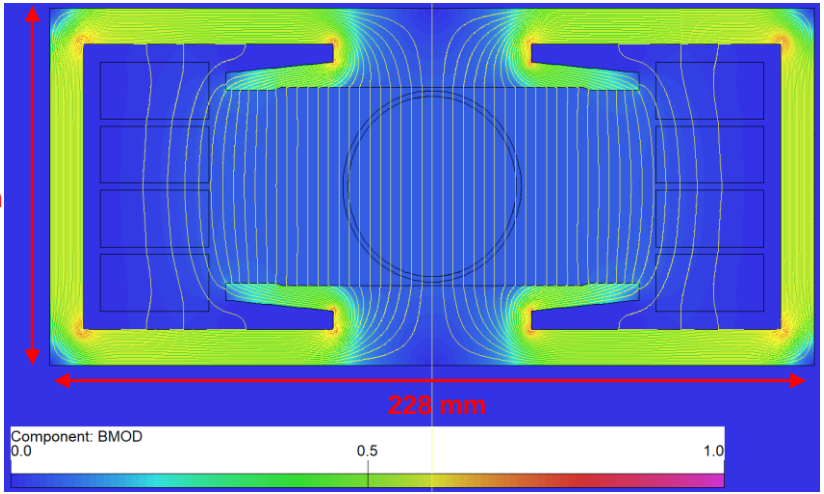

@ extraction, 182.5 GeV (tt_{bar})

- **Field quality** *(2D simulations, hysteresis not included)*
  - *Field homogeneity varies from injection to extraction energy, but is kept within ± 1.0E-4 (1 “unit”) in Ø 50 mm aperture*

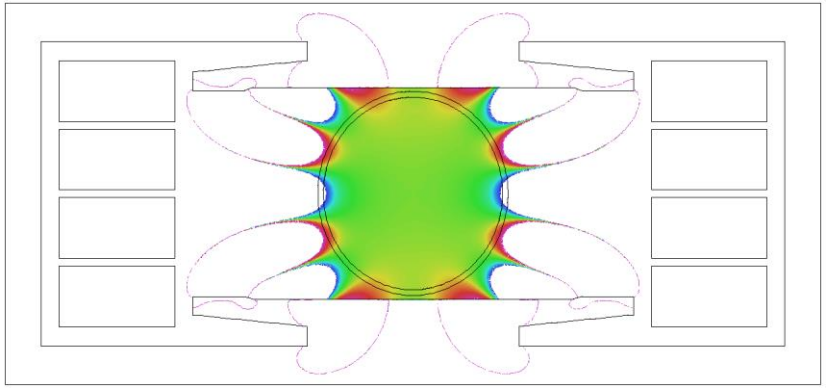

@ injection, 20 GeV

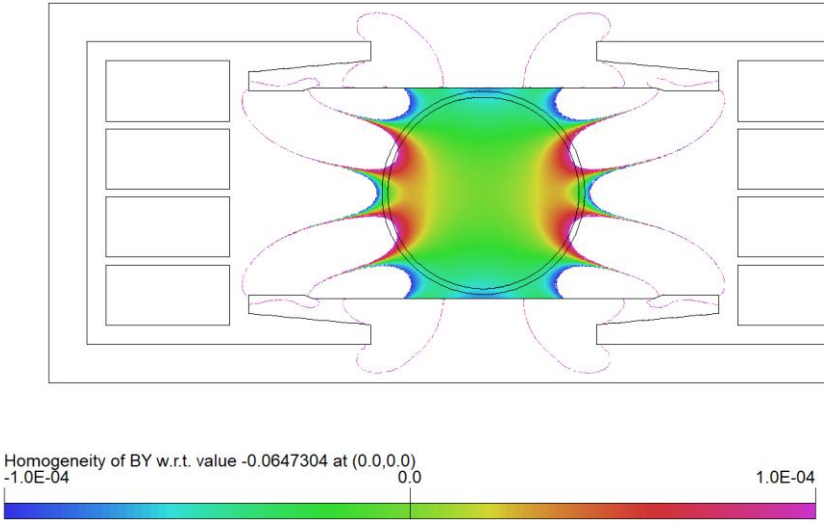

@ extraction, 182.5 GeV (tt_{bar})

- *Good margin on field homogeneity (By) at mid-plane and along specified GFR boundary*

In horizontal mid-plane

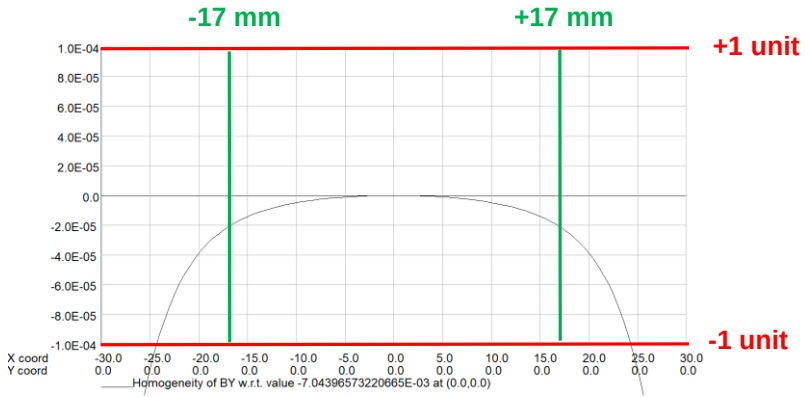

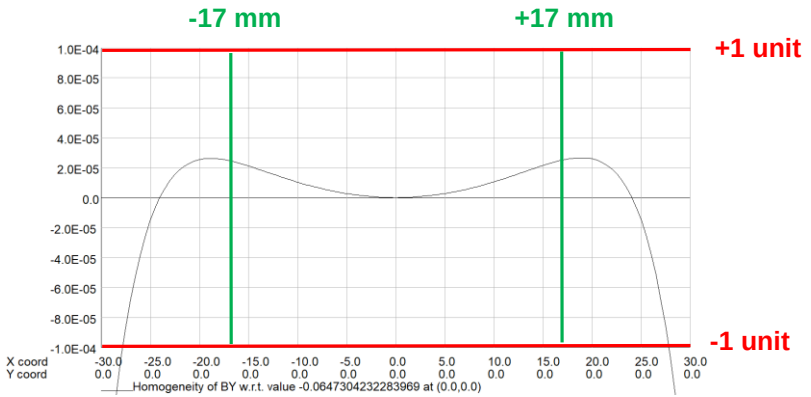

Along GFR boundary, R_{ref} = 17 mm

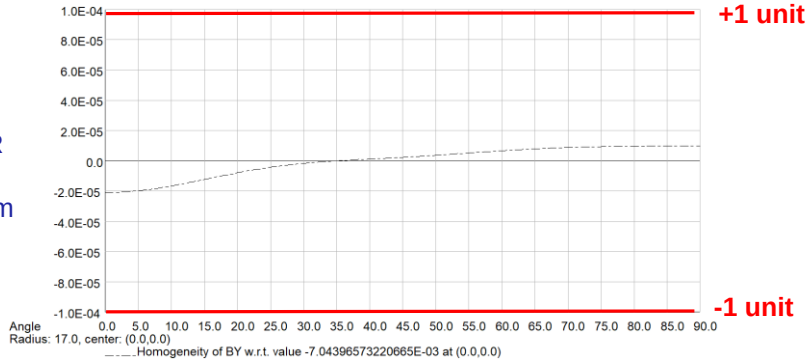

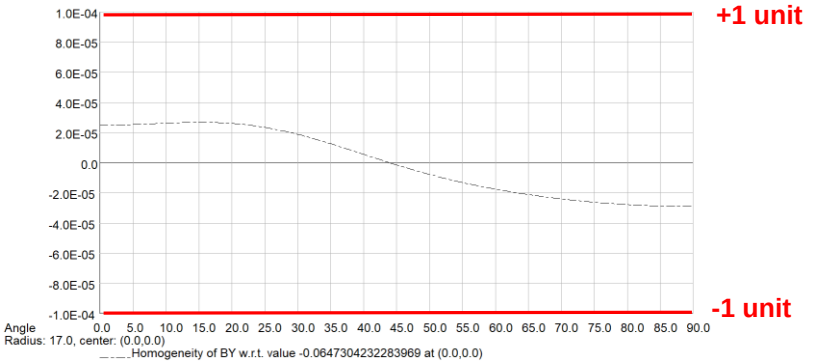

@ injection, 20 GeV

@ extraction, 182.5 GeV (tt_{bar})

- **Harmonics**
  - *All harmonics are within less than 1 unit*
  - *To be reevaluated with accurate μ_r and H_c characteristics*

Parameter	Unit	Value
Number of units		2944 x 2
Central field, 20 GeV–182.5 GeV	mT	7.1 - 65.0
Aperture (horizontal × vertical)	mm	123 x 55
Good field region (GFR) radius	mm	17
Field quality in GFR	1.0E-04	< 1
Magnetic length	m	11.1
Magnet overall transverse dimensions	mm	228 x 100
Iron mass per unit length	kg/m	55.5
Aluminium mass per unit length	kg/m	7.68
Magnet unit mass (11.1 m length)	kg	701
Total magnet mass, 65.4 km	tons	~ 4500
Maximum operating ampere-turns (tt_bar extraction)	A	2844
Maximum RMS current density (tt_bar)	A/mm2	0.92
Peak current (coil 4 turns)	*A*	*711*
Resistance per unit length (coil 4 turns)	*μΩ/m*	*596*
Inductance per unit length (coil 4 turns)	*μH/m*	*55*
Peak voltage per 1/2 octant (coil 4 turns)	*kV*	*1810*
Maximum RMS power per unit length (tt_bar)	W/m	64
Maximum total peak power, 65.4 km (tt_bar; cabling not incl.)	MW	20
Maximum total RMS power, 65.4 km (tt_bar; cabling not incl.)	MW	4.2

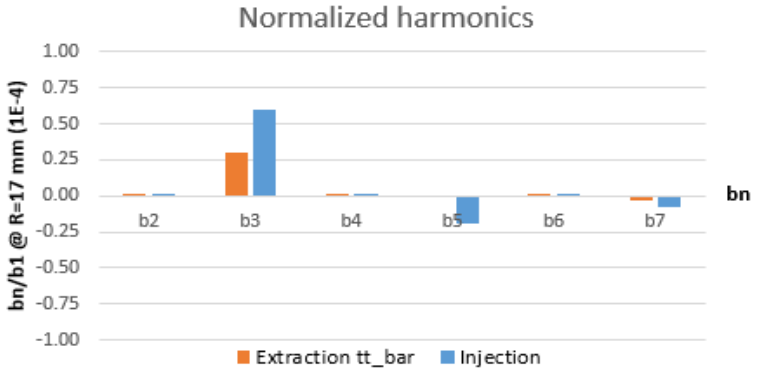

- **Parameters list**
  - *Only **~4500 tons** of iron and aluminum for the 5888 dipoles of the whole ring (~1/3 of the collider dipoles)*
  - *Power consumption minimized with **low current density***
  - *Max RMS power **~4.2 MW** (without cabling) only reached during tt_{bar} operation, will scale by order(s) of magnitude at other machine stages*
  - *Coil number of turns to optimize the matching with the converters, aiming at operational voltage **< 1 kV** in the machine (**electrical safety regulations**)*

Magnet Work Package

Prospects for the Magnet Work Package

- Design work for collider magnets
  - *Mechanical design and integration of **interconnections** (dipole **cross-section update**)*
  - *Optimization of **quadrupole** magnet to address **magnetic axis shift***
  - ***Sextupole** conceptual design with correction circuits (→ **collaboration**)*
- Design work for booster magnets
  - *Studies for **hysteretic behaviour of dipole** (simulations + experimental model magnet)*
  - *Design of **quadrupole** (in progress) and **sextupole** (to start)*
- Arc cell-mock-up
  - ***Mechanical design** of magnets and **prototypes** construction*
  - ***Large series manufacturing** challenges*

→ **We welcome collaboration proposals** to support our magnet development work!

Conclusions

Conclusions

Detailed mechanical design and integration studies of components in the magnet interconnections are needed to confirm present design baseline (e.g. inter-beam distance)

The collider quadrupole design has to be reviewed to address the magnetic axis shift generated by the aperture coupling

A collaboration agreement is under preparation for the development of the collider sextupole magnet

A compact low consumption iron dominated magnet design seems a good option for the booster dipole. Its performance in the low fields needs further study and experimental confirmation with measurements on model magnets

References

1. *A. Milanese*, "Efficient twin aperture magnets for the future circular e+/e- collider," Phys. Rev. Accel. Beams, vol. 19, 2016, Art. no. 112401.
2. *A. Milanese and M. Bohdanowicz*, "Twin aperture bending magnets and quadrupoles for FCC-ee," IEEE Trans. Appl. Supercond., vol. 28, no. 3, Apr. 2018, Art. no. 4000904.
3. *A. Milanese, C. Petrone, J. Bauche*, "Magnetic Measurements of the First Short Models of Twin Aperture Magnets for FCC-ee," IEEE Trans. Appl. Supercond., vol. 30, 2020, Art. no. 4003905.
4. *M. Benedikt et al.*, "Future circular collider conceptual design report, vol. 2: The lepton collider (FCC-ee)," Eur. Phys. J. ST., vol. 228, no. 2, 2019.
5. *D. Schoerling*, "Case study of a magnetic system for low-energy machines," Phys. Rev. Accel. Beams, vol. 19, 2016, Art. no. 082401.
6. *J. P. Gourber and L. Resegotti*, "Implication of the low field levels in the LEP magnets", IEEE Trans. Nucl. Sci. 26, 3185 (1979).
7. *D. Tommasini, M. Buzio, and R. Chritin*, "Dipole magnets for the LHeC ring-ring option", IEEE Trans. Appl. Supercond. 22, 4000203 (2012).

FCC

Thank you for your attention!

Questions?